

Clinical Observations in Rare Sinonasal Schwannoma-Clinical Case with A Literary Review

Lena Marinova^{1*}, Vaska Vassileva¹, Iliya Gabrovski¹, Bistra Yordanova²

¹Department of Radiation Oncology and Metabolic Brachytherapy, Medical Oncology Clinic, UMHAT “Queen Joanna” Sofia, Bulgaria.

²Department of Clinical Pathology, Complex Oncology Center, Ruse, Bulgaria.

*Corresponding author

Lena Marinova, Department of Radiation Oncology and Metabolic Brachytherapy, Medical Oncology Clinic, UMHAT “Queen Joanna” Sofia, Bulgaria.

Submitted: 05 Sep 2022; Accepted: 11 Sep 2022; Published: 22 Sep 2022

Citation: Lena Marinova, Vaska Vassileva, Iliya Gabrovski, Bistra Yordanova (2022) Clinical observations in rare sinonasal Schwannoma-clinical case with a literary review. *Medical & Clinical Research* 7(9):1-8.

Abstract

Schwannoma is a benign, encapsulated, slow-growing and generally solitary tumour that arise from Schwann cells of the peripheral nerve sheath. Sinonasal schwannoma is a rare entity represent less than four percent of all tumors in the head and neck area. We present our clinical observations in a 57-year-old woman with a locally advanced sinonasal schwannoma, originating in the sphenoid sinus and infiltrating ethmoid cells, the nasal cavity and the left retrobulbar space. Histopathological and immunohistochemical examination confirmed the diagnosis. Differential diagnosis requires a broad immunohistochemical analysis that will differentiate schwannoma from other benign and malignant peripheral nerve sheath tumors. Our clinical observations show that the only effective treatment of patients with schwannoma is a radical tumor surgery, as it concerns an extremely radioresistance benign tumor.

Keywords: Sinonasal Schwannoma, Pathohistological Analysis, Immunohistochemical Analysis, Surgery, Radioresistance Benign Tumor

Introduction

Schwannoma is a benign, encapsulated, slow-growing and generally solitary tumour that arise from Schwann cells of the peripheral nerve sheath [1-4]. This tumor was first described by Verocay in 1910, who coined the term “neurilemmoma” to describe this benign neurogenic tumor [5]. Schwannomas are among the most common of the peripheral nerve sheath tumors, which include neurofibromas, perineuriomas, granular cell tumors and malignant peripheral nerve sheath tumors [2]. Schwannoma can be found at any age, although most commonly found between the 3rd and 6th decades, and it has no gender preference [6]. Extracranial schwannomas in the head and neck region comprise 25-45% of all schwannomas, but only 4% involve the nasal cavity and paranasal sinuses [3,7-9]. The diagnosis of this benign tumor is extremely difficult and requires pathohistological analysis and a widely immunohistochemical examination. We will present our observations on the difficult diagnosis of sinonasal schwannoma, its slow clinical expansion, symptoms and the necessary treatment.

Clinical Case

A 57-year-old patients with headaches, progressive unilateral nasal obstruction, decrease of visual acuity of the left eye and visible left exophthalmus are presented.

From CT/December 2020 with no visible focal nodular lesions in the brain parenchyma supratentorial in the two large brain hemispheres, intratentorial at the level of the trunk and in the cerebellar hemispheres. Without pathological deviation on the part of the ventricular system with normointensity ventricular volumes. No CT data on extra and intracerebral blood collections. Normal image of the basal tanks. Subarachnoid spaces along the cranial convexity are undisturbed. Calcifications in the pineal gland, choroid plexuses of the two trigonums and in falx cerebri. Free chiasm tank. Free retrobulbar space on the right. At the base of the left retrobulbar space with data on the presence of a small irregularly shaped area with a compacted and thickened medial rectus eye muscle. The soft tissue tumor bilaterally at the base of the ethmoid sinuses and rhinobase with osteolytic changes in

the clivus and complete involvement of sphenoid sinuses. Soft tissue formations at the base of the nasal cavity on the right with dimensions 8 mm/5 mm and left 5 mm/6 mm. Hyperplasia of the two maxillary sinuses to a mild degree. Free frontal sinuses (Figure 1).

MRI/March 2021 The brain substance of T2-FLAIR and other sequences are with isointense signal without changes in the brain ventricles. The pituitary gland has a preserved structure and sizes. Rightly, a 14 mm/6 mm soft tissue formation is visualized, destroying adjacent bones, engaging the sphenoid sinus and ethmoid sinuses bilateral, entering the two nasal passages, more in the right, and infiltrating the left retrobulbar space (Figure 2 A,B,C). March 2021 an endonasal biopsy with a histological result an inflammatory myofibroblastic tumor was performed. From the immunohistochemical (IHC) examination-spindle cells express Vimentin, do not expose ALK 1; About 10% of plasmocytes expose the IG G4. Due to the diagnosis of a slow growing border tumor, the patient is evaluated for active monitoring. In April 2021, the patient was reenforced to perform endoscopic medial orbital decompression.

Local Status A pronounced exophthalmus on the left eye. Hyperemated and leaked nasal mucosa, without possible inspection in the nasal cavity. Not palpated enlarged cervical lymph nodes bilaterally.

Intraoperative After the opening of the left maxillary sinus, an anterior and posterior ethmoidectomy was performed, as a large part of the ethmoid cells were destroyed and infiltrated by the tumor. The tumor originates from the sphenoid sinus on the right, destroying the adjacent bones and engaging bilateral ethmoid cells, enters the two nasal passages, more to the right and extends to the left retrobulbar space. It reached the anterior wall of the sphenoid sinus, whose bone is infiltrated by the tumor. The sphenoid sinus opened and cleaned from the tumor to the rhinobase. Moderate bleeding was manifested, and after stopping it moved to endoscopic medial decompression of the orbit of the left eye. The lamina papyracea was removed and an incision of periorbital tissue was performed. Sent material for histological examination from the anterior wall of the sphenoid sinus to the left and from the periorbital tumor tissue to the left.

Consultation of the histological result the material represents bone fragments and tumor proliferation with the following characteristics: 1/Biphasic cell proliferation; 2/Spindel schwannoma cell (fascicular scar) and vacuolized areas; 3/The cells have unclearly distinguished cytoplasm, dense chromatin, without axons; 4/No mitotic figures are observed; 5/Degenerative changes/hyalinization (Figures 3-5).

From Immunohistochemical (IHC) Analysis Tumor cells with positive expression to the S100 Protein and Vimentin (Figure 6A, B), and in single atypical cells there is a positive expression to CD 117 (Figure 7A/B). Focal positive SMA expression of single fibroblasts localized around the positive SMA walls of blood vessels (Figure 7C/D). Figure 8A presents tumor cells with negative

expression to CK AE1/AE3; negative expression to Desmin and to Myogenin (Figure 8B/C). Only the walls of the blood vessels and scattered cells in Antoni B areas are marked to the CD 34. (Figure 8D) In Figures 9 we present Antoni A area with cellular appearance with several rows of palisaded nuclei (outlined with red rectangles) and Antoni B area with pale mucinous stroma which has few cells, scattered wispy collagen and mast cells tagged with Vimentin/outlined with the yellow rectangle (Figure 9A/D). The tumor cells are negative to CD 34, tightly arranged around the blood vessels/shown with yellow arrows (Figure 9B), single Interstitial Cajal-Like cells positive to CD117 (Figure 9C). After nonradical surgery, the patient is evaluated for active monitoring. Given the benign nature of the disease and its slow growth, the patient is not directed for radiotherapy (RT). After a year of partial surgery, complaints of headaches and secretions from the nasal cavity are restored, and the vision of the left eye with exophthalm completely disappears. MRI January 2022 visualizes a soft tissue tumor engaging the sphenoid sinus and ethmoidal sinuses bilateral, which destroys the adjacent bones and enters the two nasal passages and infiltrates the left retrobulbar space (Figure 10). Due to the available symptoms, it was estimated to carry out intensity modulated radiotherapy (IMRT) in the tumor area with a daily dose (DD) 2 Gy up to total dose (TD) 66 Gy (Figures 11,12). The patient has suffered RT without radiation reactions. After 3 months, a control MRI was conducted to establish tumor stationation, lack of visible reduction or progression (Figure 13). After 6 months after the end of RT, the patient is in good general condition, without symptoms and of good quality of life. It is subject to active monitoring.

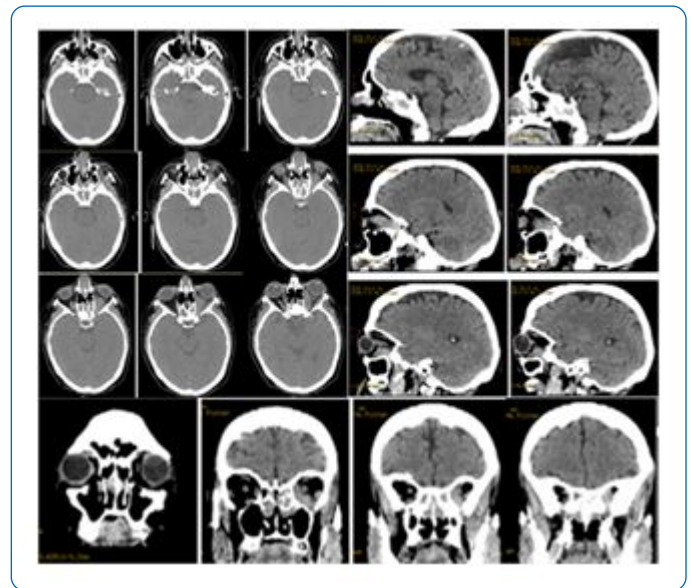


Figure 1: CT/December 2020. The soft tissue tumor bilaterally at the base of the ethmoid sinuses and rhinobase with osteolytic changes in the clivus and complete involvement of sphenoid sinuses. The tumor covers the base of the nasal cavity on the right with dimensions 8 mm/5 mm and left 5 mm/6 mm. Hyperplasia of the two maxillary sinuses to a mild degree.

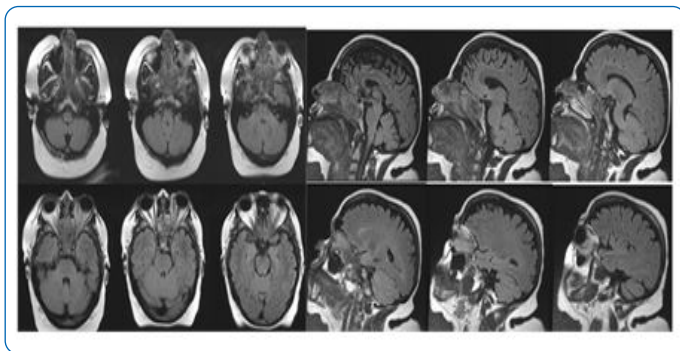


Figure 2: A/B Axial and sagittal MRI/March 2021. The brain substance of T2-FLAIR and other sequences are with isointense signal without changes in the brain ventricles. Rightly, a 14 mm/6 mm soft-tissue formation is visualized, destroying adjacent bones, engaging the sphenoid sinus and ethmoid sinuses bilateral, entering the two nasal passages, more in the right, and infiltrating

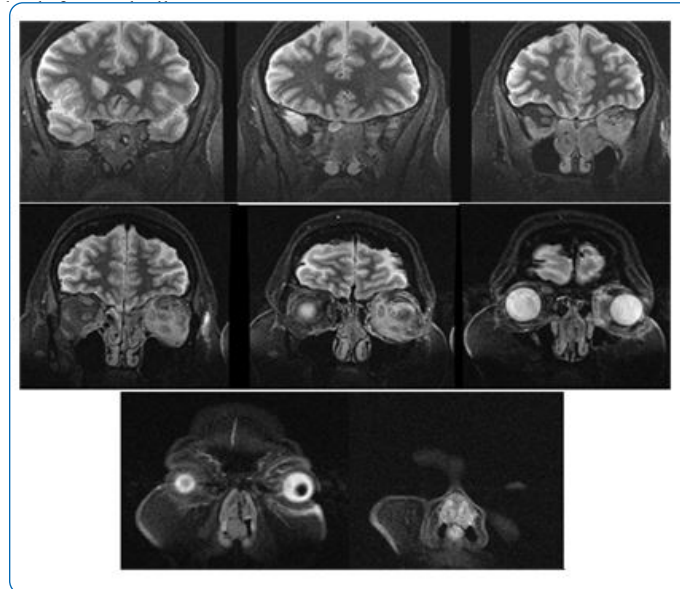


Figure 2: C) Coronal MRI/March 2021. The brain substance of T2-FLAIR and other sequences are with isointense signal without changes in the brain ventricles. The pituitary gland has a preserved structure and sizes. Rightly, a 14 mm/6 mm soft-tissue formation is visualized, destroying adjacent bones, engaging the sphenoid sinus and ethmoid sinuses bilateral, entering the two nasal passages, more in the right, and infiltrating the left retrobulbar space.

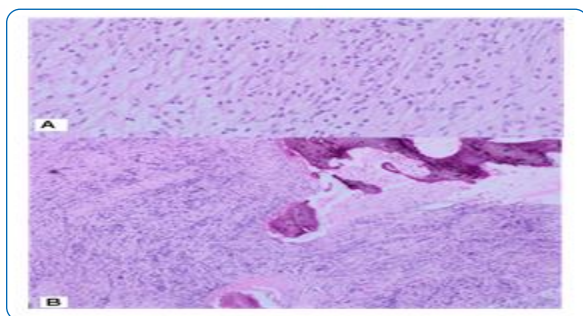


Figure 3: Microscopic histological findings. A) Tumor cells have ill defined cytoplasm and dense chromatin pattern H&E x 40; B)

Spindle cells show interlacing pattern and palisading of nuclei with expressed hyalinization of tumor stroma; Bone structures are visualized at the top right, and below to the right whorling pattern H&E x 20.

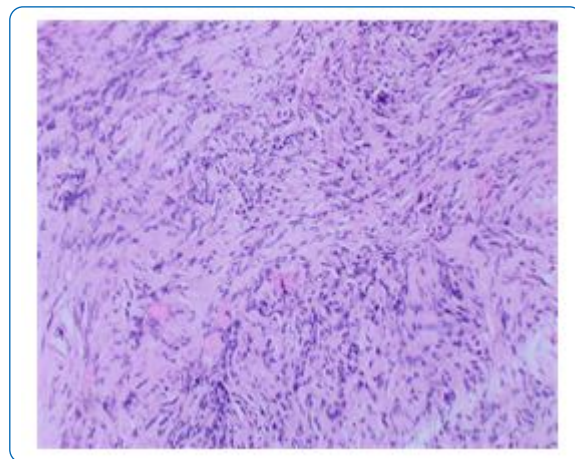


Figure 4: Microscopic histological findings. Areas with many cells and a small amount of cells; Spindle cells show interlacing pattern and palisading of nuclei; whorling pattern on the right; expressed hyalinization of tumor stroma. H&E x 100.

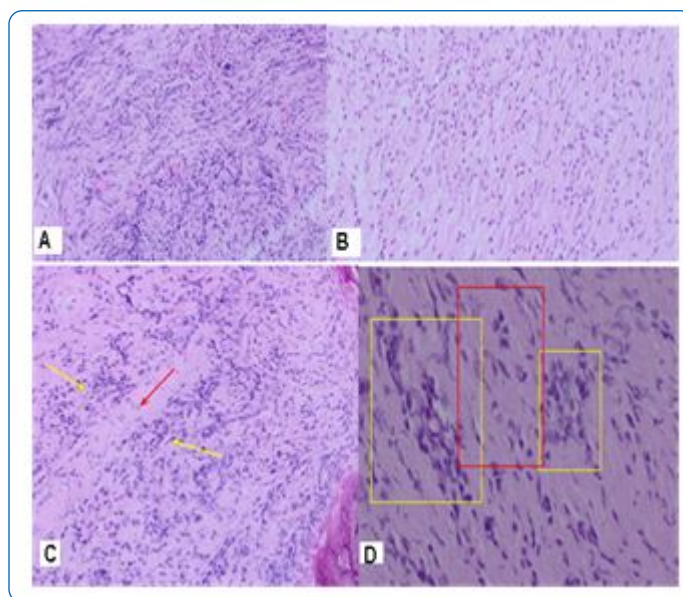


Figure 5: Microscopic histological findings. A) Spindle cells show interlacing pattern and palisading of nuclei; whorling pattern on the right H&E x 20; B) Cells are narrow, elongated and wavy with tapered ends interspersed with collagen fibers H&E x 20; C) At high power (H&E x 40) the palisading nuclei and Verocay bodies are evident, as well as the Antony A and Antony B components (the yellow arrows show Antony A and Antony B components, and the red arrow shows parallel arrays of nuclei forming a Verocay body); D) At high power (H&E x 100) the palisading nuclei and Verocay bodies are evident, as well as the Antony A and Antony B components (the yellow rectangles show Antony A and Antony B components, and the red shows parallel arrays of nuclei forming a Verocay body).

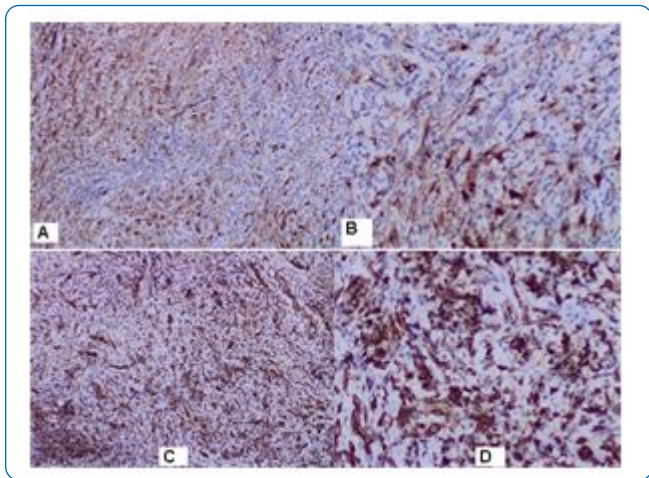


Figure 6: Immunohistochemistry. A/B) Tumor cells with positive expression to S100 protein (at low power H&E x 100 and at high power H&E x 400); C/D) Tumor cells with positive Vimentin expression (at low power H&E x 100 and at high power H&E x 400).

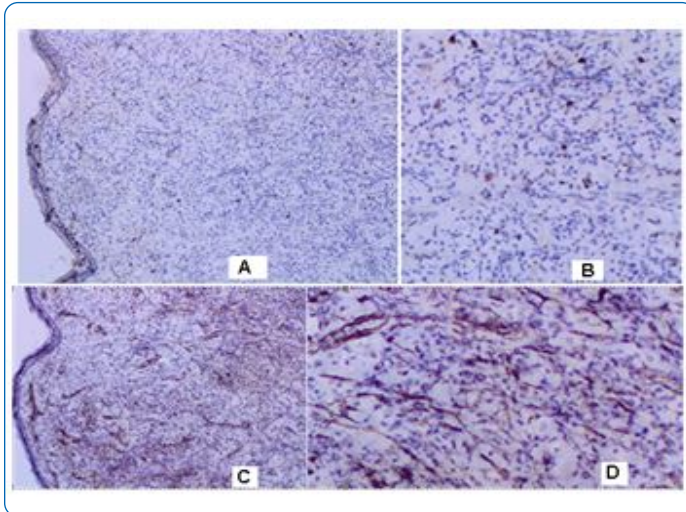


Figure 7: Immunohistochemistry. A/B) Single atypical cells there is a positive expression to CD 117 (at low power H&E x 40 and at high power H&E x 100); C/D) Focal positive SMA expression of single fibroblasts localized around the positive SMA walls of blood vessels (at low power H&E x 40 and at high power (H&E x 100).

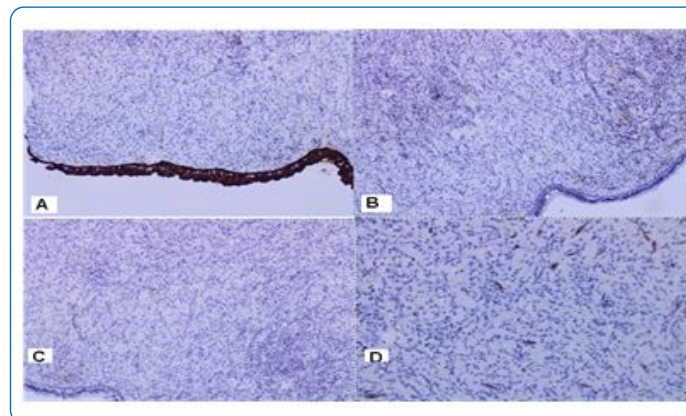


Figure 8: Immunohistochemistry. A) Tumor cells with negative CK AE1/AE3 expression; B) Negative expression to Desmin; C) Negative expression to Myogenin; D) Only the walls of the blood vessels and scattered cells in Antoni B areas are marked to the CD 34.

CK AE1/AE3 expression; B) Negative expression to Desmin; C) Negative expression to Myogenin; D) Only the walls of the blood vessels and scattered cells in Antoni B areas are marked to the CD 34.

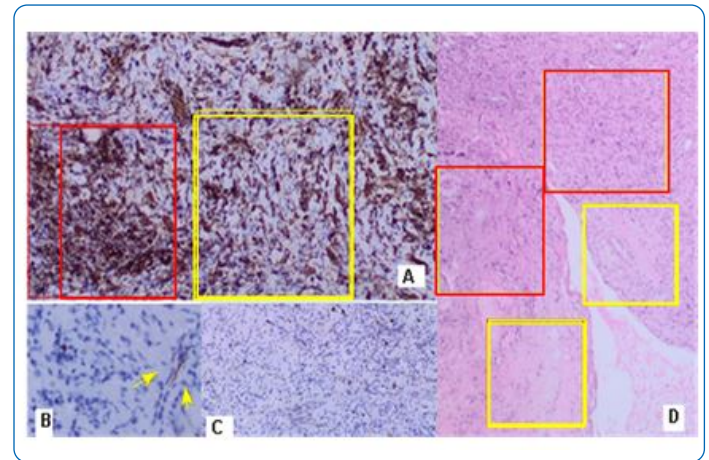


Figure 9: Immunohistochemistry and microscopic histological findings. A/D) Antoni A area with cellular appearance with several rows of palisaded nuclei (outlined with red rectangles) and Antoni B area with pale mucinous stroma which has few cells, scattered wispy collagen and mast cells tagged with Vimentin (outlined with the yellow rectangle). A) Tagged with Vimentin; D/ H&E x 40; B) The tumor cells are negative to CD 34, tightly arranged around the blood vessels/shown with yellow arrows; C) Single Interstitial Cajal-Like Cells positive to CD117+.

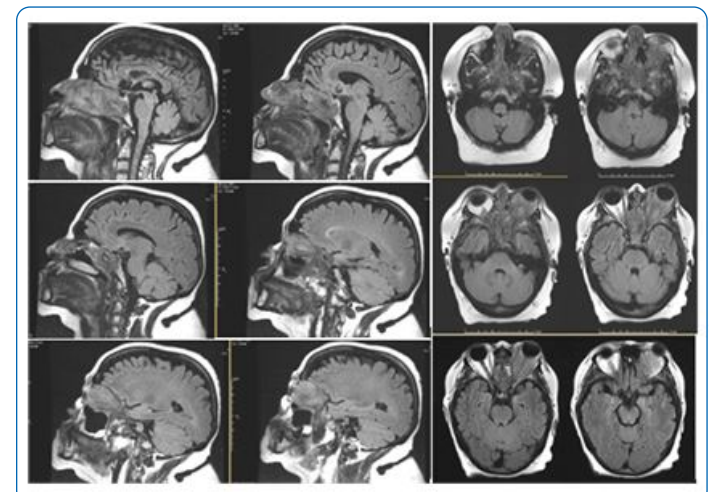


Figure 10: MRI/January 2022. Sag T2 FLAIR and AxT2 FLAIR visualizes a soft tissue tumor engaging bilateral the sphenoid sinus and ethmoidal sinuses, which destroys the adjacent bones and enters the two nasal passages and infiltrates the left retrobulbar space.

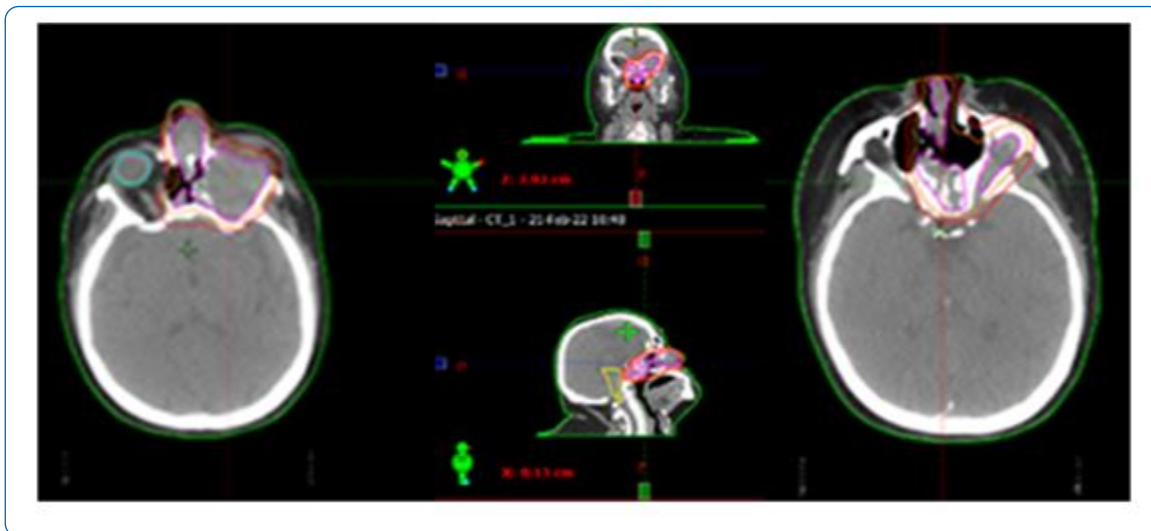


Figure 11: Preparation of radiation treatment by determining the target volume and contouring the adjacent normal tissues and organs.

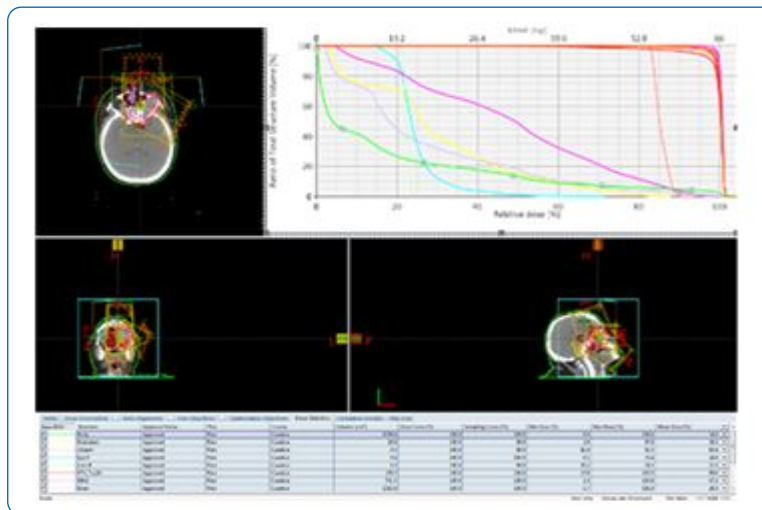


Figure 12: Intensity modulated radiotherapy by the VMAT method in the tumor area with a daily dose 2 Gy up to total dose 66 Gy

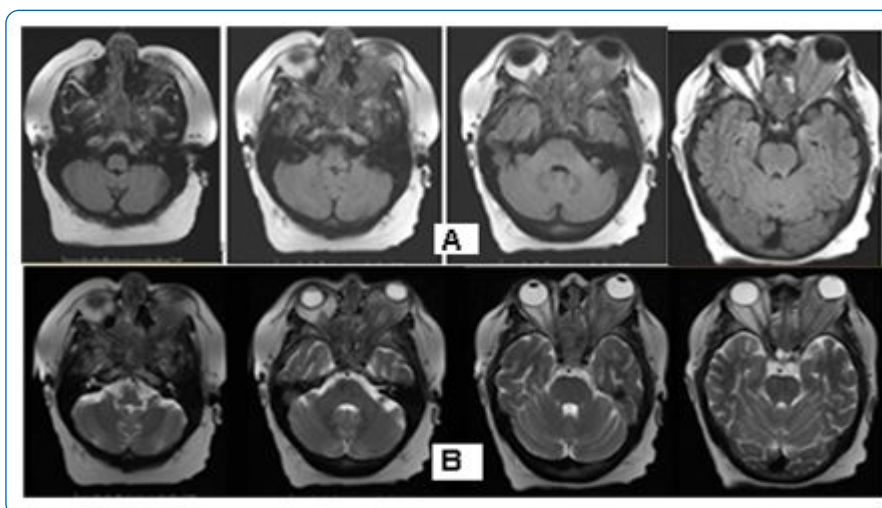


Figure 13: MRI 3 months after the completion of the radiation treatment of tumor stationarity without reduction or progression. A) Ax T2 FLAIR B) Ax T2 FRFSE.

Discussion

Schwannomas are benign, well-circumscribed tumors usually attached to peripheral nerves, consisting of a clonal population of Schwann cells, which often undergo cystic and degenerative change [2]. These tumors can emerge from any nerve covered with a Schwann cell sheath, including the cranial nerves (with the exception of the optic and olfactory nerves), the spinal nerves, and the autonomous nervous system [10]. Apart from cranial nerves, schwannomas may be observed in other sites, such as the tongue [1], stomach [11], colon [12], knee [13] and penis [14]. In sinonasal cavity, schwannomas are postulated to arise from the ophthalmic and maxillary branches of the trigeminal nerve or from autonomic nerves to the septal vessels and mucosa [15]. The ethmoid is the most common site of rhinosinusal location, followed by the maxillary sinus, the nasal cavity, and the sphenoid [16].

Sinonasal region, even though it is located in the head, has an extremely low incidence (about 4%) of Schwannomas [9,17]. They have a variety of morphological appearances, but they behave as World Health Organization (WHO) grade I tumors [2]. Malignant transformation within a schwannoma usually results in an epithelioid or primitive neuroectodermal morphology [18,19].

Pre-operative diagnosis is difficult and further investigations are needed such as MRI, CT, US and angiography [20]. On a contrast CT scan, schwannoma of the tongue exhibits heterogeneous enhancement [21]. CT shows usually a round homogeneous density lesion, without calcification generally [22]. Since they have a tendency to grow slowly, the adjacent osseous structures remodeling can be secondary to benign pressure erosion [23]. In our clinical case, the CT reports a soft-tissue tumor with a homogeneous structure that destroys adjacent bone, which is typical of slow-growing tumors (Figure 1). The typical features on MRI are a well-circumscribed small nodule, homogeneously isointense to muscle on T1WI and homogeneously hyperintense on T2WI, showing homogeneous enhancement after contrast administration [24]. In the presented clinical case, MR T2 FLAIR images of the tumor are isointense to muscle tissue (Figures 2A-C, Figure 10 and 13). The clinical and imaging differential diagnosis for a sinonasal mass would include squamous carcinoma, adenocarcinoma, lymphoma, esthesioneuroblastoma, meningioma, as well as an aggressive fungal infection [25]. Histopathological and immunohistochemical examination confirmed the diagnosis [1]. The histopathological material represents tumor proliferation with the following characteristics: 1/biphasic cell proliferation (cellular Antoni A & hypocellular Antoni B); 2/Spindel schwannoma cell (fascicular scar) and vacuolized areas; 3/The cells with unclearly distinguished cytoplasm, dense chromatin, axons generally absent within lesion; 4/No mitotic figures are observed; 5/Degenerative changes /hyalinization. (Figure 3 and Figure 5A,B). Microscopically, schwannomas are well circumscribed, with a surrounding capsule, and contain areas composed of fascicles of Schwann cells that have a spindle cell morphology (Antoni A pattern), which may either merge with or abruptly change to other more loosely textured and microcystic areas (Antoni B pattern) [1,2]. The characteristic of Antoni A is extended spindle-shaped cells with elongated nuclei, arranged in bundles, drifts, and

whorls, and Verocay bodies, while hypocellular Antoni B areas present very loose tissue composed by polymorphism of cells and abundant myxoid [3,23]. Cellular schwannoma is defined as a schwannoma composed almost entirely of a compact, fascicular proliferation of well-differentiated, cytologically bland Schwann cells, lacking Verocay bodies [26,27]. Verocay in 1910 [28], first described the structure that was later eponymically named Verocay body and is considered diagnostic of a schwannoma. A typical Verocay body consists of a stacked arrangement of two rows of elongated palisading nuclei that alternates with acellular zones made up of cytoplasmic processes of the Schwann cells [4]. The histological diagnosis of schwannoma is usually apparent because of the presence of alternating patterns of Antoni A and B areas, nuclear palisading, Verocay bodies, and the whirling of cells, histological finding that we present in Figure 5C, D and Figure 9A, D. The immunohistochemical examination revealed positivity for vimentin, S-100 and glial fibrillary acidic protein, whereas discovered on GIST-1, CD117, CD34, desmin, smooth muscle actin (SMA) and cytokeratin were negative [29]. Schwannomas are characterized by strong and diffuse immunoreactivity for S-100 protein, which is the clue for the diagnosis [30-32]. The presence of S-100 protein in IHC staining is a classic marker for diagnostic confirmation and magnetic resonance imaging (MRI) is the gold standard for preoperative imaging [33]. There is some truth to the contention that schwannomas express S100 to a greater extent than neurofibromas, but because of a degree of overlap in the expression of this marker between these two tumors, relying on this stain alone is not sufficient [34]. In our clinical case, we report a positive expression of tumor cells to S100 protein and Vimentin (Figure 6), single atypical cells with positive expression to CD 117 (Figure 7A, B). Importantly, cellular schwannomas lack expression of smooth muscle actin, desmin, CD117 and DOG1, allowing exclusion of other important tumors in its differential diagnosis, leiomyosarcoma and GIST, respectively [35]. An interesting immunohistochemical finding is the positive SMA expression except in the walls of the blood vessels and in single fibroblasts localized around them (Figure 7C, D). The presence of alpha-SMA in benign neoplasms and in well-differentiated leiomyosarcomas suggests that this actin isoform reflects a high degree of cellular differentiation [36]. Due to the positive expression of single cells to the SMA, a differential diagnosis with leiomyomas is required, but they are characterized by a negative S100 protein expression [37]. Superficial leiomyoma is a benign dermal smooth muscle neoplasm, often arising from arrector pili (pilo-leiomyoma), which is characterized by a positive SMA, MSA, Desmin IHC expression [38]. Figure 8A represents tumor cells with negative CK AE1/AE3 expression and a well visible spinocellular epithelium; negative expression to Desmin and to Myogenin (Figure 8B/C) Only the walls of the blood vessels and scattered cells in Antoni B areas are marked to the CD 34 (Figure 8D). CD34 is a useful stain for differential diagnosis between neurofibromas and shwannomas, since neurofibromas typically demonstrate a significant subpopulation of CD34-positive stromal cells, unlike most schwannomas [34]. Peripheral nerve sheath tumors encompass a spectrum of well defined clinicopathologic entities [39], ranging from benign tumors, such as schwannoma, to high grade malignant neoplasms termed malignant peripheral nerve

sheath tumors (MPNST), which are often resistant to conventional treatments [40]. As schwannomas are typically benign, well circumscribed, and minimally invasive tumors, complete surgical excision is the standard of care for ensuring no recurrence [41-45]. The surgical techniques used varied according to time, before the year 2000 the surgeries were performed using an external approach or a combination of an external and endonasal approach [46]. In our clinical case, intraoperatively observed destroying the adject bones, which is also visible to MRI. This bone change is not a sign of tumor malignancy, but the result of its slow growth, leading to erosion of adjacent cranial bones. These tumours do not respond to radiotherapy [47]. In our clinical case, it is a locally advanced sinonasal schwannoma originating in the sphenoid sinus and the engagement of the clivus, which defines the tumor as a inoperable. After decompressive surgery, the tumor continues to grow slowly. After a year, it provokes symptomatic that requires decompressive radiotherapy. Due to the tumor radioresistance, we conducted IMRT to a high radical dose-TD 66 Gy (Figure 12). After 3 months a control MRI was carried out, which was reported to the stationing of the available tumor, without visible reduction or progression (Figure 13). Our clinical observations show that the only effective treatment in schwannoma is a radical tumor surgery, as it concerns an extremely radioresistance benign tumor. Despite the rarity of malignant transformation, long-term monitoring is usually necessary [48,49]. Recurrence, metastasis or malignant degeneration did not occur after surgical removal in any of the six cases, as it was verified by a follow-up of 2 to 5 years [50].

Conclusion

Schwannoma is a benign, encapsulated, slow-growing and generally solitary tumour that arise from Schwann cells of the peripheral nerve sheath. Histopathological and immunohistochemical examination confirmed the diagnosis. Differential diagnosis requires a broad immunohistochemical analysis that will differentiate schwannoma from other benign and malignant peripheral nerve sheath tumors. Radical surgery is the only effective treatment for local tumor control and prolonged survival. The tumor is radioresistance and the realization of a high radiation dose can only lead to its stationation, lack of visible reduction or progression.

References

- Abreu I, Roriz D, Rodrigues P, Moreira A, Marques C, Alves FC (2017) Schwannoma of the tongue-A common tumour in a rare location: A case report. *Eur J Radiol Open* 4: 1-3.
- Hilton DA, Hanemann CO (2014) Schwannomas and their pathogenesis. *Brain Pathol* 24: 205-220.
- Santosh Kumar S, Smrutipragnya S, Somadatta D, Rabindranath P (2021) A Large Intraoral Sublingual Schwannoma in a Pediatric Patient: A Case Report *Iran J Otorhinolaryngol* 33(118): 335-337.
- Rajiv J (2012) Learning from eponyms: Jose Verocay and Verocay bodies, Antoni A and B areas, Nils Antoni and Schwannomas. *Indian Dermatol Online J* 3(3):215-219.
- Lollar WK, Pollak N, Liess DB (2010) Schwannoma of the hard palate. *Am J Otolaryngol* 31(2): 139-140.
- Kavcic J, Bozic M (2016) Schwannoma of the tongue. *BMJ Case Rep* 1-4.
- Berlusconi M, Piazza C, Blanzuoli L, Battaglia G, Nicolai P (2000) Schwannoma of the nasal septum: a case report with review of the literature. *Eur Arch Otorhinolaryngol* 257: 402-405.
- A El-Saggan, J Olofsson, B Krossnes (2003) Sinonasal schwannoma: two case reports and review of literature. *Int Congress Series* 1240: 503-507.
- Buob D, Wacrenier A, Chevalier D, Aubert S, Quinchon JF, et al. (2003) Schwannoma of the sinonasal tract: a clinicopathologic and immunohistochemical study of 5 cases *Arch Pathol Lab Med* 127 (9): 1196-1199.
- Harada H, Omura K, Maeda A (2001) A massive pleomorphic adenoma of the submandibular salivary gland accompanied by neurilemmomas of the neck misdiagnosed as a malignant tumor: report of case. *J Oral Maxillofacial Sur* 59(8):931-935.
- Romdhane H, Cheikh M, Mzoughi Z, et al. (2016) Gastric Schwannoma: A Case Report. *Clin Pract* 6: 849.
- Wang WB, Chen WB, Lin JJ, Xu JH, Wang JH, et al. (2016) Schwannoma of the colon: A case report and review of the literature. *Oncol Lett* 11: 2580-2582.
- Oz TT, Aktas B, Ozkan K, Ozturan B, Kilic B, et al.(2017) A Case of Schwannoma of the Common Peroneal Nerve in the Knee. *Orthop Rev (Pavia)* 9: 6825.
- Loeser A, Katzenberger T, Meuller JG, Riedmiller H, Gerharz EW, et al. (2007) Solitary schwannoma of the glans penis. *Urology* 70: 1007.e5-1007.e6.
- Hegazy HM, Snyderman CH, Fan CY, Kassam AB (2001) Neurilemmomas of the paranasal sinuses. *Am J Otolaryngol* 22: 215-218.
- Sheikh HY, Chakravarthy RP, Slevin NJ, Sykes AJ, Banerjee SS (2008) Benign schwannoma in paranasal sinuses: A clinicopathological study of five cases, emphasising diagnostic difficulties. *J Laryngol Otol* 122: 598-602.
- Hillstrom RP, Zarbo RJ, Jacobs JR (1990) Nerve sheath tumors of the paranasal sinuses: electron microscopy and histopathologic diagnosis. *Otolaryngology Head Neck Surg* 102 (3): 257-263.
- McMenamin ME, Fletcher CD (2001) Expanding the spectrum of malignant change in schwannomas: epithelioid malignant change, epithelioid malignant peripheral nerve sheath tumor, and epithelioid angiosarcoma: a study of 17 cases. *Am J Surg Pathol* 25: 13-25.
- Woodruff JM, Selig AM, Crowley K, Allen PW (1994) Schwannoma (neurilemoma) with malignant transformation. A rare, distinctive peripheral nerve tumor. *Am J Surg Pathol* 18:882-895
- Boccolini C, Cavazza S, Laudadio P (2005) Schwannoma of cervical sympathetic chain: assessment and management. *Acta Otorhinolaryngol Ital* 25(3): 191-194.
- Fang WS, Wiggins RH, Illner A, Hamilton BE, Hedlund GL, et al. (2011) Primary lesions of the root of the tongue. *Radiographics* 31(7): 1907-1922.
- Bentao Y, Zhenchang W, Sha L, et al. (2008) CT and MRI appearance of schwannoma in the sinonasal region. *Chinese J Radiology* 42 (6): 618-622.
- Ma XH, Zhou HC, Lai C, Zhu K, Jia X (2016) Pediatric Isolated Sinonasal Schwannoma: A New Case Report and

- Literature Review. Case Rep Med 2016:2786030.
24. Cohen M, Wang B (2009) Schwannoma of the tongue: two case reports and review of the literature. Eur Arch Otorhinolaryngol 266: 1823-1829.
 25. Yu E, Mikulis D, Nag S (2006) CT and MR imaging findings in sinonasal schwannoma. AJNR Am J Neuroradiol 27: 929-930.
 26. Fletcher CD, Davies SE, McKee PH (1987) Cellular schwannoma: a distinct pseudosarcomatous entity. Histopathol 11: 21-35.
 27. White W, Shiu MH, Rosenblum MK, Erlandson RA, Woodruff JM (1990) Cellular schwannoma. A clinicopathologic study of 57 patients and 58 tumors. Cancer 66: 1266-1275.
 28. Verocay J (1910) [Zur Kenntnis der 'neurofibrome. Beitr Pathol Anat 48: 1-69.
 29. An X, Zhu M, Zhang N, Lu S, Wei P, et al. (2017) Schwannoma of the vagina-a common tumor but a rare location: A case report. Mol Clin Oncol 7(5): 783-786.
 30. Fisher C (2011) 2nd edition. Amirsys; Diagnostic Pathology: Soft Tissue Tumors.
 31. Lindberg MR (2016) 2nd edition. Amirsys; Diagnostic Pathology: Soft Tissue Tumors.
 32. Weiss SW, Nickoloff BJ (1993) CD-34 is expressed by a distinctive cell population in peripheral nerve, nerve sheath tumors, and related lesions. Am J Surg Pathol 17: 1039-1045.
 33. Singh GB, Arora R, Garg S, Aggarwal K (2015) Base of tongue schwannoma. ENT-Ear, Nose & Throat J 306-308
 34. Rodney T (2007) Miller Immunohistochemistry in the Differential Diagnosis of Schwannoma and Neurofibroma Immunohistochemistry Newsletter.
 35. Rodriguez FJ, Folpe AL, Giannini C, Perry A (2012) Pathology of peripheral nerve sheath tumors: diagnostic overview and update on selected diagnostic problems. Acta Neuropathol 123(3): 295-319.
 36. Schürch W, Skalli O, Seemayer TA, Gabbiani G (1987) Intermediate filament proteins and actin isoforms as markers for soft tissue tumor differentiation and origin. I. Smooth muscle tumors. Am J Pathol 128(1):91-103.
 37. <https://www.pathologyoutlines.com/topic/softtissueleiomyomadeep.html>.
 38. Magro G (2018) Differential Diagnosis of Benign Spindle Cell Lesions. Surg Pathol Clin 11(1): 91-121.
 39. Louis DN, Ohgaki H, Wiestler OD, Cavenee WK, editors (2007) WHO Classification of Tumours of the Central Nervous System. International Agency for Research on Cancer; Lyon.
 40. Slomiany MG, Dai L, Bomar PA, Knackstedt TJ, Kranc DA, et al. (2009) Abrogating drug resistance in malignant peripheral nerve sheath tumors by disrupting hyaluronan-CD44 interactions with small hyaluronan oligosaccharides. Cancer Res 69: 4992-4998.
 41. Mehrzad H, Persaud R, Papadimitriou N, Kaniyur S, Mochloulis G (2006) Schwannoma of tongue base treated with transoral carbon dioxide laser. Lasers Med Sci 21(04): 235-237.
 42. Rathore AS, Srivastava D, Narwal N, Shetty DC (2015) Neurilemmoma of Retromolar Region in the oral cavity. Case Rep Dent 2015: 320830.
 43. Biswas D, Marnane CN, Mal R, Baldwin D (2007) Extracranial head and neck schwannomas-a 10-year review. Auris Nasus Larynx 34: 353-359.
 44. Melvin WS, Wilkinson MG (1993) Gastric schwannoma. Clinical and pathologic considerations. Am Surg 59: 293-296.
 45. Pasquini E, Sciarretta V, Farneti G, Ippolito A, Mazzatenta D, et al. (2002) Endoscopic endonasal approach for the treatment of benign schwannoma of the sinonasal tract and pterygopalatine fossa. Am J Rhinol 16: 113-118.
 46. Riveros AC, Proietti V, Serrano C, Ruggerics (2021) Sinonadal Schwannomas. J Otolaryngol Rhinol 7: 108.
 47. Sutay S, Tekinsoy B, Ceryan K, Aksu Y (1993) Submaxillary hypoglossal neuri-lemmoma. J Laryngol Otol 107: 953-954.
 48. Kandasamy S, Nathan RS, John RR (2017) Neurilemmoma of maxillary alveolus: a rare case report and review of literature. J Pharm Bioallied Sci 9(1): 285-288.
 49. Sethi D, Sethi A, Nigam S, Agarwal A (2008) Schwannoma of oral tongue: a rare benign neoplasm. The Int J Head Neck Surgery 3(1): 84-96.
 50. Pantazopoulos P (2009) Schwannoma of nose, oral cavity, and pharynx. Acta Oto-Laryngologica 60: 97-104.

Copyright: ©2022: Lena Marinova, et al. This is an open-access article distributed under the terms of the Creative Commons Attribution License, which permits unrestricted use, distribution, and reproduction in any medium, provided the original author and source are credited.